Fully heavy tetraquark states and their evidences in LHC observations

Ming-Sheng Liu,[1,4] Feng-Xiao Liu,[1,5,*] Xian-Hui Zhong,[1,5,†] and Qiang Zhao[2,3,5,‡]

[1]*Department of Physics, Hunan Normal University, and Key Laboratory of Low-Dimensional Quantum Structures and Quantum Control of Ministry of Education, Changsha 410081, China*
[2]*Institute of High Energy Physics, Chinese Academy of Sciences, Beijing 100049, China*
[3]*University of Chinese Academy of Sciences, Beijing 100049, China*
[4]*College of Science, Tianjin University of Technology, Tianjin 300384, China*
[5]*Synergetic Innovation Center for Quantum Effects and Applications (SICQEA), Hunan Normal University, Changsha 410081, China*

Stimulated by the exciting progress on the observations of the fully charmed tetraquarks at LHC, we carry out a combined analysis of the mass spectra and fall-apart decays of the 1S-, 2S-, and 1P-wave $cc\bar{c}\bar{c}$ states in a nonrelativistic quark model. It is found that the $X(6600)$ structure observed in the di-J/ψ invariant mass spectrum can be explained by the 1S-wave state $T_{(4c)0^{++}}(6550)$. This structure may also bear some feed-down effects from the higher 2S and/or 1P tetraquark states. The $X(6900)$ structure observed in both the di-J/ψ and $J/\psi\psi(2S)$ channels can be naturally explained by the 2S-wave state $T_{(4c)0^{++}}(6957)$. The small shoulder structure around 6.2–6.4 GeV observed at CMS and ATLAS may be due to the feed-down effects from some 1P-wave states with $C = -1$ and/or some 2S-wave states with $J^{PC} = 0^{++}$. Other decay channels are implied in such a scenario and they can be investigated by future experimental analyses. Considering the large discovery potential at LHC, we also present predictions for the $bb\bar{b}\bar{b}$ states which can be searched for in the future.

I. INTRODUCTION

Searching for genuine exotic hadrons beyond the conventional quark model has been one of the most important initiatives since the establishment of the nonrelativistic constituent quark model in 1964 [1,2]. Benefited from great progresses in experiment, many candidates of exotic hadrons have been found since the discovery of $X(3872)$ by Belle in 2003 [3]. Recent reviews of the status of experimental and theoretical studies can be found in Refs. [4–10]. While many observed candidates have been found located in the vicinity of S-wave open thresholds, no signals for overall-color-singlet multiquark states have been indisputably established due to difficulties of distinguishing them from hadronic molecules [10]. Recently, the tetraquarks of all-heavy systems, such as $cc\bar{c}\bar{c}$ and

$bb\bar{b}\bar{b}$, have received considerable attention. Since the light quark degrees of freedom cannot be exchanged between two heavy mesons at leading order, the color interactions between the heavy quarks (antiquarks) should be dominant at short distance and they may favor to form genuine color-singlet tetraquark configurations rather than loosely bound hadronic molecules. Furthermore, such exotic states may have masses and decay modes significantly different from other conventional states, thus, can be established in experiment.

Early theoretical studies of the full heavy tetraquark states can be found in the literature [11–16]. A revival of this topic driven by the experimental progresses can be found by the intensive publications recently [17–37]. Physicists are very concerned with the stability of the tetraquark $cc\bar{c}\bar{c}$ ($T_{(4c)}$) and $bb\bar{b}\bar{b}$ ($T_{(4b)}$) states. If the $T_{(4c)}$ or $T_{(4b)}$ states have relatively smaller masses below the thresholds of heavy charmonium or bottomonium pairs [18–25], they may become "stable" because no direct decays into heavy quarkonium pairs through quark rearrangements would be allowed. However, some studies showed that stable bound tetraquark states made of $cc\bar{c}\bar{c}$ or $bb\bar{b}\bar{b}$ may not exist [11,15,27–35] because the predicted masses are large enough for them to decay into heavy quarkonium pairs. Due to these very controversial issues, experimental evidence for such exotic objects would

be crucial for our understanding of the underlying dynamics.

In 2020, the LHCb Collaboration reported their results on the observations of $T_{(4c)}$ states [38]. In the di-J/ψ invariant mass spectrum, a broad structure above $J/\psi J/\psi$ threshold ranging from 6.2 GeV to 6.8 GeV and a narrower resonance $X(6900)$ were observed with more than 5σ of significance level. There are also some vague structures around 7.2 GeV to be confirmed. Later in 2022, $X(6900)$ was confirmed in the same final state by both the ATLAS [39] and CMS [40] Collaborations. Some signal of $X(6900)$ was also seen in the $J/\psi\psi(2S)$ channel by the ATLAS Collaboration [39]. In addition, in the lower-mass region the CMS measurements show that a clear resonance $X(6600)$ together with a small shoulder structure around 6.2–6.4 GeV lies in the di-J/ψ spectrum [40]. These clear structures may be evidences for genuine tetraquark $T_{(4c)}$ states, they can also set up experimental constraints on theoretical models of which the successful interpretations and most importantly the early predictions should bring a lot of insights to the underlying dynamics. Stimulated by the newly observed structures in the di-J/ψ invariant mass spectrum, the study of full heavy tetraquark states has been a hot topic in the last two years [41–92].

In Refs. [33,93] we adopted a nonrelativistic potential quark model (NRPQM), which is based on the Hamiltonian proposed by the Cornell model [94], for the study of fully heavy tetraquark system. The masses of the $1S$-wave fully-heavy tetraquark states were predicted there and we found that the $1S$-wave $T_{(4c)}$ masses should be above the two-charmonium thresholds within a commonly accepted parameter space [33]. This turns out to be consistent with the structure $X(6600)$. The predicted masses of the $2S$-wave $T_{(4c)}$ states are comparable with the narrow structure $X(6900)$. Later studies by Refs. [35,55–57,95] turn out to agree with our predictions.

In this work we carry out a systematic study of the fall-apart decays of the $1S$-, $2S$-, and $1P$-wave $T_{(4Q)}$ states in the NRPQM framework. The $1S$-, $2S$-, and $1P$-wave $T_{(4Q)}$ ($Q = c, b$) states are calculated in the same framework. Thus, it allows us to obtain a self-consistent treatment for the mass spectrum and decay properties. We will show that some of these structures observed at LHC may arise from the S- and P-wave $T_{(4c)}$ states. To proceed, we first give a brief introduction to our model and method.

II. MODEL AND METHOD

Apart from the linear confinement, Coulomb type potential, and spin-spin interaction potential for calculating the S-wave tetraquark states in the Hamiltonian [33], we include the spin-orbit and tensor potentials here to deal with the first orbital ($1P$) excitation,

$$V_{ij}^{LS} = -\frac{\alpha_{ij}}{16}\frac{\lambda_i \cdot \lambda_j}{r_{ij}^3}\left(\frac{1}{m_i^2} + \frac{1}{m_j^2} + \frac{4}{m_i m_j}\right)\{\mathbf{L}_{ij} \cdot (\mathbf{S}_i + \mathbf{S}_j)\}$$
$$- \frac{\alpha_{ij}}{16}\frac{\lambda_i \cdot \lambda_j}{r_{ij}^3}\left(\frac{1}{m_i^2} - \frac{1}{m_j^2}\right)\{\mathbf{L}_{ij} \cdot (\mathbf{S}_i - \mathbf{S}_j)\}, \quad (1)$$

$$V_{ij}^T = -\frac{\alpha_{ij}}{4}(\lambda_i \cdot \lambda_j)\frac{1}{m_i m_j r_{ij}^3}\left\{\frac{3(\mathbf{S}_i \cdot \mathbf{r}_{ij})(\mathbf{S}_j \cdot \mathbf{r}_{ij})}{r_{ij}^2} - \mathbf{S}_i \cdot \mathbf{S}_j\right\}, \quad (2)$$

where $r_{ij} \equiv |\mathbf{r}_i - \mathbf{r}_j|$ is the distance between the ith and jth quarks, $\mathbf{S}_i$ stands for the spin of the ith quark, and $\mathbf{L}_{ij}$ stands for the relative orbital angular momentum between the i-th and j-th quark. If the interaction occurs between two quarks or antiquarks, operator $\lambda_i \cdot \lambda_j$ is defined as $\lambda_i \cdot \lambda_j \equiv \sum_{a=1}^{8} \lambda_i^a \lambda_j^a$, while if the interaction occurs between a quark and antiquark, we have $\lambda_i \cdot \lambda_j \equiv \sum_{a=1}^{8} -\lambda_i^a \lambda_j^{a*}$, where λ^{a*} is the complex conjugate of the Gell-Mann matrix λ^a. The parameters b_{ij} and α_{ij} denote the confinement potential strength and the strong coupling for the OGE potential, respectively. The same model parameters, $m_c/m_b = 1.483/4.852$ GeV, $\alpha_{cc}/\alpha_{bb} = 0.5461/0.4311$, $\sigma_{cc}/\sigma_{bb} = 1.1384/2.3200$ GeV, and $b_{cc/bb} = 0.1425$ GeV^2, are adopted by fitting the $c\bar{c}$ and $b\bar{b}$ spectra as in Refs. [33,96].

For $T_{(4Q)}$, there are two kinds of color structures, $(6\bar{6})_c$ and $(3\bar{3})_c$. As shown in Fig. 1, the relative Jacobi coordinate between these two charm quarks (two anticharm quarks) is defined by $\boldsymbol{\xi}_1 = (\mathbf{r}_1 - \mathbf{r}_2)/\sqrt{2}$ ($\boldsymbol{\xi}_2 = (\mathbf{r}_3 - \mathbf{r}_4)/\sqrt{2}$), while the relative Jacobi coordinate between $Q_1 Q_2$ and $\bar{Q}_3 \bar{Q}_4$ is defined by $\boldsymbol{\xi}_3 = (\mathbf{r}_1 + \mathbf{r}_2)/2 - (\mathbf{r}_3 + \mathbf{r}_4)/2$. Thus, there are three spatial excitation modes which are denoted as ξ_1, ξ_2, and ξ_3. Their wave functions are defined as $\phi(\xi_i)$ ($i = 1, 2, 3$). According to the requirements of
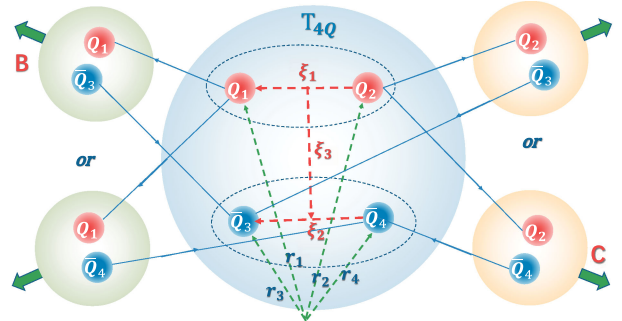

FIG. 1. The coordinates defined for a $T_{(4Q)}$ system and its fall-apart decays into a BC meson pair via the quark rearrangement. The BC final state can be formed via two quark rearrangement ways: $(Q_1\bar{Q}_3)(Q_2\bar{Q}_4)$ and $(Q_1\bar{Q}_4)(Q_2\bar{Q}_3)$ as shown in the figure.
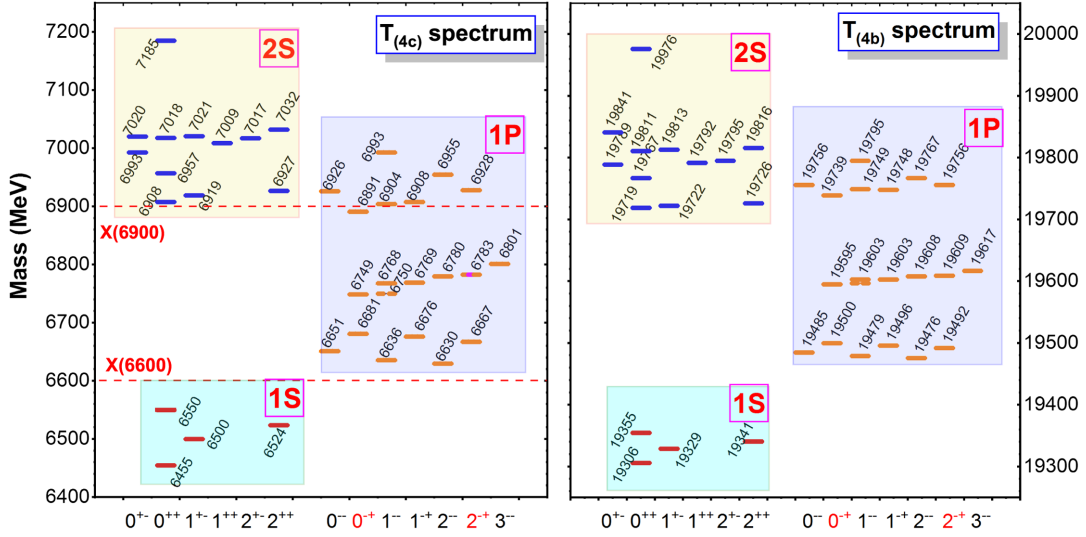
symmetry, there will be four $1S$ configurations, 12 $2S$ configurations, and 20 $1P$ configurations in the $L-S$ coupling scheme, which are listed in Table I. Apart from the conventional quantum numbers, i.e., $J^{PC} = 0^{-+}$, $1^{--}, 2^{-\pm}, 3^{--}$, the P-wave states can access exotic quantum numbers, i.e., $J^{PC} = 0^{--}, 1^{-+}$.

To solve the Schrödinger equation, we expand the radial part $R_{n_{\xi_i} l_{\xi_i}}(\boldsymbol{\xi_i})$ of spatial wave function $\phi(\xi_i)$ with a series of harmonic oscillator functions [97],

$$R_{n_{\xi_i} l_{\xi_i}}(\xi_i) = \sum_{\ell=1}^{n} \mathcal{C}_{\xi_i \ell} \phi_{n_{\xi_i} l_{\xi_i}}(d_{\xi_i \ell}, \xi_i), \qquad (3)$$

TABLE I. Mass spectra for the $1S, 1P, 2S$-wave $cc\bar{c}\bar{c}$ and $bb\bar{b}\bar{b}$ states. ξ_1, ξ_2, ξ_3 are the Jacobi coordinates. (ξ_1, ξ_2) stands for a configuration containing both ξ_1- and ξ_2-mode orbital excitations, while (ξ_3) stands for a configuration containing ξ_3-mode orbital excitation. The spectra for the $1S$ and $2S$ states are taken from our previous works [33,93].

Configuration	$cc\bar{c}\bar{c}$ Eigenvector	Mass (MeV)	$bb\bar{b}\bar{b}$ Eigenvector	Mass (MeV)
$1^1S_{0^{++}(6\bar{6})_c}$ $1^1S_{0^{++}(\bar{3}3)_c}$	$\begin{pmatrix} 0.58 & 0.81 \\ 0.81 & -0.58 \end{pmatrix}$	$\begin{pmatrix} 6455 \\ 6550 \end{pmatrix}$	$\begin{pmatrix} 0.58 & 0.81 \\ 0.81 & -0.58 \end{pmatrix}$	$\begin{pmatrix} 19306 \\ 19355 \end{pmatrix}$
$1^3S_{1^{+-}(\bar{3}3)_c}$	1	6500	1	19329
$1^5S_{2^{++}(\bar{3}3)_c}$	1	6524	1	19341
$^3P_{0^{--}(6\bar{6})_c(\xi_1,\xi_2)}$ $^3P_{0^{--}(\bar{3}3)_c(\xi_1,\xi_2)}$	$\begin{pmatrix} -0.80 & 0.60 \\ 0.60 & 0.80 \end{pmatrix}$	$\begin{pmatrix} 6651 \\ 6926 \end{pmatrix}$	$\begin{pmatrix} -0.81 & 0.59 \\ 0.59 & 0.81 \end{pmatrix}$	$\begin{pmatrix} 19485 \\ 19756 \end{pmatrix}$
$^3P_{0^{-+}(6\bar{6})_c(\xi_1,\xi_2)}$ $^3P_{0^{-+}(\bar{3}3)_c(\xi_1,\xi_2)}$ $^3P_{0^{-+}(\bar{3}3)_c(\xi_3)}$	$\begin{pmatrix} 0.82 & 0.47 & 0.32 \\ 0.14 & 0.38 & -0.91 \\ -0.55 & 0.80 & 0.25 \end{pmatrix}$	$\begin{pmatrix} 6681 \\ 6749 \\ 6891 \end{pmatrix}$	$\begin{pmatrix} 0.82 & 0.55 & 0.12 \\ 0.02 & 0.18 & -0.98 \\ -0.57 & 0.81 & 0.14 \end{pmatrix}$	$\begin{pmatrix} 19500 \\ 19595 \\ 19739 \end{pmatrix}$
$^3P_{1^{--}(6\bar{6})_c(\xi_1,\xi_2)}$ $^3P_{1^{--}(\bar{3}3)_c(\xi_1,\xi_2)}$ $^5P_{1^{--}(\bar{3}3)_c(\xi_3)}$ $^1P_{1^{--}(\bar{3}3)_c(\xi_3)}$ $^1P_{1^{--}(6\bar{6})_c(\xi_3)}$	$\begin{pmatrix} -0.82 & 0.55 & 0.12 & -0.06 & 0.03 \\ 0.02 & -0.24 & 0.96 & -0.16 & 0.06 \\ -0.01 & 0.05 & 0.17 & 0.98 & 0.10 \\ 0.48 & 0.69 & 0.19 & -0.02 & -0.50 \\ 0.31 & 0.39 & 0.02 & -0.11 & 0.86 \end{pmatrix}$	$\begin{pmatrix} 6636 \\ 6750 \\ 6768 \\ 6904 \\ 6993 \end{pmatrix}$	$\begin{pmatrix} -0.82 & 0.57 & 0.06 & -0.03 & 0.01 \\ 0.00 & -0.10 & 0.98 & -0.18 & 0.02 \\ 0.00 & 0.03 & 0.18 & 0.98 & 0.04 \\ 0.53 & 0.76 & 0.08 & -0.02 & -0.36 \\ 0.22 & 0.28 & 0.00 & -0.05 & 0.93 \end{pmatrix}$	$\begin{pmatrix} 19479 \\ 19597 \\ 19603 \\ 19749 \\ 19795 \end{pmatrix}$
$^3P_{1^{-+}(6\bar{6})_c(\xi_1,\xi_2)}$ $^3P_{1^{-+}(\bar{3}3)_c(\xi_1,\xi_2)}$ $^3P_{1^{-+}(\bar{3}3)_c(\xi_3)}$	$\begin{pmatrix} 0.82 & 0.56 & 0.05 \\ 0.01 & 0.08 & -1.00 \\ -0.57 & 0.82 & 0.06 \end{pmatrix}$	$\begin{pmatrix} 6676 \\ 6769 \\ 6908 \end{pmatrix}$	$\begin{pmatrix} 0.82 & 0.57 & 0.05 \\ 0.00 & 0.08 & -1.00 \\ -0.57 & 0.82 & 0.06 \end{pmatrix}$	$\begin{pmatrix} 19496 \\ 19603 \\ 19748 \end{pmatrix}$
$^3P_{2^{--}(6\bar{6})_c(\xi_1,\xi_2)}$ $^3P_{2^{--}(\bar{3}3)_c(\xi_1,\xi_2)}$ $^5P_{2^{--}(\bar{3}3)_c(\xi_3)}$	$\begin{pmatrix} 0.80 & -0.59 & -0.06 \\ 0.01 & 0.12 & -0.99 \\ 0.60 & 0.80 & 0.10 \end{pmatrix}$	$\begin{pmatrix} 6630 \\ 6780 \\ 6955 \end{pmatrix}$	$\begin{pmatrix} 0.81 & -0.59 & -0.03 \\ 0.00 & 0.06 & -1.00 \\ 0.59 & 0.81 & 0.05 \end{pmatrix}$	$\begin{pmatrix} 19476 \\ 19608 \\ 19767 \end{pmatrix}$
$^3P_{2^{-+}(6\bar{6})_c(\xi_1,\xi_2)}$ $^3P_{2^{-+}(\bar{3}3)_c(\xi_1,\xi_2)}$ $^3P_{2^{-+}(\bar{3}3)_c(\xi_3)}$	$\begin{pmatrix} 0.82 & 0.57 & -0.06 \\ 0.00 & -0.10 & -1.00 \\ -0.58 & 0.81 & -0.08 \end{pmatrix}$	$\begin{pmatrix} 6667 \\ 6783 \\ 6928 \end{pmatrix}$	$\begin{pmatrix} 0.82 & 0.58 & 0.00 \\ 0.00 & 0.00 & -1.00 \\ -0.58 & 0.82 & 0.00 \end{pmatrix}$	$\begin{pmatrix} 19492 \\ 19609 \\ 19756 \end{pmatrix}$
$^5P_{3^{--}(\bar{3}3)_c(\xi_3)}$	1	6801	1	19617
$2^1S_{0^{+-}(6\bar{6})_c(\xi_1,\xi_2)}$ $2^1S_{0^{+-}(\bar{3}3)_c(\xi_1,\xi_2)}$	$\begin{pmatrix} -0.66 & -0.75 \\ -0.75 & 0.66 \end{pmatrix}$	$\begin{pmatrix} 6993 \\ 7020 \end{pmatrix}$	$\begin{pmatrix} 0.10 & -1.00 \\ -1.00 & -0.10 \end{pmatrix}$	$\begin{pmatrix} 19789 \\ 19841 \end{pmatrix}$
$2^1S_{0^{++}(6\bar{6})_c(\xi_1,\xi_2)}$ $2^1S_{0^{++}(\bar{3}3)_c(\xi_1,\xi_2)}$ $2^1S_{0^{++}(6\bar{6})_c(\xi_3)}$ $2^1S_{0^{++}(\bar{3}3)_c(\xi_3)}$	$\begin{pmatrix} 0.35 & 0.40 & 0.03 & 0.84 \\ -0.91 & -0.05 & 0.07 & 0.41 \\ 0.21 & -0.91 & -0.01 & 0.35 \\ -0.06 & 0.02 & -1.00 & 0.05 \end{pmatrix}$	$\begin{pmatrix} 6908 \\ 6957 \\ 7018 \\ 7185 \end{pmatrix}$	$\begin{pmatrix} 0.15 & 0.38 & 0.04 & 0.91 \\ -0.97 & -0.04 & -0.14 & 0.19 \\ 0.10 & -0.92 & 0.02 & 0.37 \\ 0.14 & 0.00 & -0.99 & 0.01 \end{pmatrix}$	$\begin{pmatrix} 19719 \\ 19767 \\ 19811 \\ 19976 \end{pmatrix}$
$2^3S_{1^{+-}(\bar{3}3)_c(\xi_1,\xi_2)}$ $2^3S_{1^{+-}(\bar{3}3)_c(\xi_3)}$	$\begin{pmatrix} -0.39 & -0.92 \\ -0.92 & 0.39 \end{pmatrix}$	$\begin{pmatrix} 6919 \\ 7021 \end{pmatrix}$	$\begin{pmatrix} -0.38 & -0.92 \\ -0.92 & 0.38 \end{pmatrix}$	$\begin{pmatrix} 19722 \\ 19813 \end{pmatrix}$
$2^3S_{1^{++}(\bar{3}3)_c(\xi_1,\xi_2)}$	1	7009	1	19792
$2^5S_{2^{+-}(\bar{3}3)_c(\xi_1,\xi_2)}$	1	7017	1	19795
$2^5S_{2^{++}(\bar{3}3)_c(\xi_1,\xi_2)}$ $2^5S_{2^{++}(\bar{3}3)_c(\xi_3)}$	$\begin{pmatrix} -0.37 & -0.93 \\ -0.93 & 0.37 \end{pmatrix}$	$\begin{pmatrix} 6927 \\ 7032 \end{pmatrix}$	$\begin{pmatrix} -0.37 & -0.93 \\ -0.93 & 0.37 \end{pmatrix}$	$\begin{pmatrix} 19726 \\ 19816 \end{pmatrix}$

FIG. 2.   Mass spectra for the $cc\bar{c}\bar{c}$ and $bb\bar{b}\bar{b}$ systems.

with

$$\phi_{n_{\xi_i} l_{\xi_i}}(d_{\xi_i \ell}, \boldsymbol{\xi}_i) = \left(\frac{1}{d_{\xi_i \ell}}\right)^{\frac{3}{2}} \left[\frac{2^{l_{\xi_i}+2}}{(2l_{\xi_i}+1)!!\sqrt{\pi}}\right]^{\frac{1}{2}} \left(\frac{\xi_i}{d_{\xi_i \ell}}\right)^{l_{\xi_i}}$$
$$\times e^{-\frac{1}{2}\left(\frac{\xi_i}{d_{\xi_i \ell}}\right)^2}. \quad (4)$$

The parameter $d_{\xi \ell}$ can be related to the harmonic oscillator frequency $\omega_{\xi \ell}$ with $1/d_{\xi \ell}^2 = M_\xi \omega_{\xi \ell}$. For $T_{(4Q)}$ the reduced masses $M_{\xi_i} = m_Q$. On the other hand, the harmonic oscillator frequency $\omega_{\xi_i \ell}$ can be related to the harmonic oscillator stiffness factor K_ℓ with $\omega_{\xi_i \ell} = \sqrt{3K_\ell/M_{\xi_i}}$. Then, one has $d_{\xi_i \ell} = d_\ell = (3m_Q K_\ell)^{-1/4}$. The oscillator length d_ℓ is set to be

$$d_\ell = d_1 a^{\ell-1} \quad (\ell = 1, \ldots, n), \quad (5)$$

where n is the number of harmonic oscillator functions, and a is the ratio coefficient. There are three parameters $\{d_1, d_n, n\}$ to be determined through the variation method. It is found that with the parameter sets $\{0.068 \text{ fm}, 2.711 \text{ fm}, 15\}$ and $\{0.050 \text{ fm}, 2.016 \text{ fm}, 15\}$ for the $cc\bar{c}\bar{c}$ and $bb\bar{b}\bar{b}$ systems, we can obtain stable solutions.

By using the spectrum obtained from NRPQM, we further evaluate the fall-apart decays of the $T_{(4Q)}$ states in a quark-exchange model [98]. The interactions V_{ij} between inner quarks of final hadrons B and C may be the sources of the fall-apart decays of a $T_{(4Q)}$ state via the quark rearrangement. The decay amplitude $\mathcal{M}(A \to BC)$ of $T_{(4Q)}$ state is described by

$$\mathcal{M}(A \to BC) = -\sqrt{(2\pi)^3} \sqrt{8M_A E_B E_C} \langle BC | \sum_{i<j} V_{ij} | A \rangle, \quad (6)$$

where A stands for the initial tetraquark state, BC stands for the final hadron pair. M_A is the mass of the initial state, and E_B and E_C are the energies of the final states B and C, respectively. The decay width Γ of $A \to BC$ can be described by

$$\Gamma = \frac{1}{2J_A + 1} \frac{|\boldsymbol{p}|}{8\pi M_A^2} |\mathcal{M}(A \to BC)|^2, \quad (7)$$

where $|\boldsymbol{p}|$ is magnitude of the momentum for the final states B and C. The potentials V_{ij} ($ij \neq 13, 24$ or $ij \neq 14, 23$) between inner quarks of final hadrons B and C, as shown in Fig. 3, are taken the same as our mass calculations. The calculation of the decay amplitude for a $T_{(4Q)}$ state is indeed a tedious task, some details are given in the appendix. This model has been developed and applied to the study of the hidden-charm decay properties for the multiquark states in the literature [99–103], and a lot of inspiring results are obtained. For simplicity, the wave functions of the A, B, C hadron states are parametrized out in a single harmonic oscillator form by fitting the wave
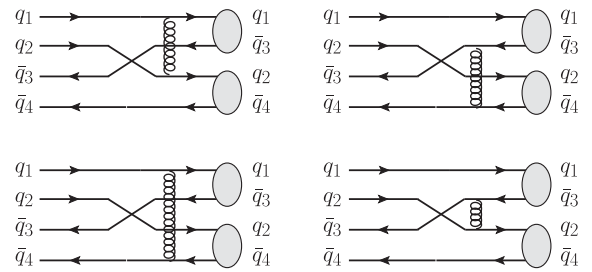
FIG. 3.   The fall-apart decays of a $T_{(4Q)}$ state induced by the interactions V_{ij} ($ij \neq 13, 24$ or $ij \neq 14, 23$) between inner quarks of final hadrons B and C.

functions calculated from our potential model [93,97,104]. The harmonic oscillator parameters for the final meson states and initial tetraquark states are collected in Tables IV and V of the Appendix, respectively.

III. RESULTS AND DISCUSSION

In Table I, the mass spectra of the $T_{(4c)}$ and $T_{(4b)}$ states are listed in the third and fifth columns, respectively.

For clarity, the mass spectra are also plotted in Fig. 2. From Table I, one can see that the physical states are usually mixtures of two different color configurations $|6\bar{6}\rangle_c$ and $|\bar{3}3\rangle_c$. The eigenvectors for different configurations of the $T_{(4Q)}$ states are also listed in Table I. The eigenvalues for the physical states can be extracted by diagonalizing the mass matrices. The masses of the 1P-wave $T_{(4c)}$ and $T_{(4b)}$ states are predicted to be in the range of $\sim$6.6–7.0 GeV

TABLE II. Fall-apart decay properties for the $T_{(4c)}$ states. The unit of the partial widths of each channel is MeV.

State	$\eta_c\eta_c$	$J/\psi J/\psi$	$\eta_c\eta_c(2S)$	$J/\psi\psi(2S)$	$\chi_{c0}\chi_{c0}/\chi_{c0}\chi_{c1}$	$\chi_{c0}\chi_{c2}/\chi_{c1}\chi_{c1}$	$\chi_{c1}\chi_{c2}/\chi_{c2}\chi_{c2}/h_c h_c$
$T_{(4c)0^{++}}(6455)(1S)$	1.45	0.70	$\cdots$	$\cdots$	$\cdots$	$\cdots$	$\cdots$
$T_{(4c)0^{++}}(6550)(1S)$	0.12	1.78	$\cdots$	$\cdots$	$\cdots$	$\cdots$	$\cdots$
$T_{(4c)2^{++}}(6524)(1S)$	$\cdots$	0.00	$\cdots$	$\cdots$	$\cdots$	$\cdots$	$\cdots$
$T_{(4c)0^{++}}(6908)(2S)$	0.61	0.12	0.55	0.09	22.5/$\cdots$	$\cdots$	$\cdots$
$T_{(4c)0^{++}}(6957)(2S)$	0.01	4.66	0.05	3.17	70.8/$\cdots$	$\cdots$	$\cdots$
$T_{(4c)0^{++}}(7018)(2S)$	3.14	1.87	0.00	0.07	14.8/$\cdots$	0.00/$\cdots$	$\cdots$
$T_{(4c)0^{++}}(7185)(2S)$	0.00	0.48	0.21	0.14	1.14/$\cdots$	0.05/6.12	0.53/18.0/5.79
$T_{(4c)2^{++}}(6927)(2S)$	$\cdots$	0.36	$\cdots$	0.30	0.00/1.15	$\cdots$	$\cdots$
$T_{(4c)2^{++}}(7032)(2S)$	$\cdots$	7.12	$\cdots$	2.83	0.23/98.0	325/214	$\cdots$

State	$J/\psi J/\psi$	$\eta_c\chi_{c0}$	$\eta_c\chi_{c1}$	$\eta_c\chi_{c2}$	$J/\psi h_c$	$J/\psi\psi(2S)/\eta_c\eta_c(2S)$	$\chi_{c0}\chi_{c0}/\chi_{c0}\chi_{c1}/\chi_{c0}\chi_{c2}$
$T_{(4c)1^{++}}(7009)(2S)$	$\cdots$	2.43	4.57	4.81	3.79	0.00/$\cdots$	$\cdots$/0.00/0.00
$T_{(4c)0^{-+}}(6681)(1P)$	0.04	1.28	0.00	0.03	0.40	$\cdots$	$\cdots$
$T_{(4c)0^{-+}}(6749)(1P)$	1.56	0.00	0.00	0.00	5.33	$\cdots$	$\cdots$
$T_{(4c)0^{-+}}(6891)(1P)$	0.00	2.38	0.00	0.79	0.06	0.00/$\cdots$	0.00/$\cdots$/$\cdots$
$T_{(4c)1^{-+}}(6676)(1P)$	0.09	0.00	1.99	0.03	1.70	$\cdots$/0.00	$\cdots$
$T_{(4c)1^{-+}}(6769)(1P)$	0.21	0.00	1.22	0.06	5.57	$\cdots$/0.00	$\cdots$
$T_{(4c)1^{-+}}(6908)(1P)$	0.00	0.00	1.43	0.06	0.37	0.00/0.00	0.31/$\cdots$/$\cdots$
$T_{(4c)2^{-+}}(6667)(1P)$	0.00	0.02	0.03	0.05	0.03	$\cdots$	$\cdots$
$T_{(4c)2^{-+}}(6783)(1P)$	0.01	0.05	0.07	1.10	2.18	$\cdots$	$\cdots$
$T_{(4c)2^{-+}}(6928)(1P)$	0.01	0.05	0.08	0.88	1.98	0.00/$\cdots$	0.00/$\cdots$/$\cdots$

state	$\eta_c J/\psi$	$\eta_c h_c$	$\chi_{c0}J/\psi$	$\chi_{c1}J/\psi$	$\chi_{c2}J/\psi$	$\eta_c\psi(2S)/\eta_c(2S)J/\psi$	$\chi_{c0}h_c$
$T_{(4c)1^{+-}}(6500)(1S)$	0.45	$\cdots$	$\cdots$	$\cdots$	$\cdots$	$\cdots$/$\cdots$	$\cdots$
$T_{(4c)0^{+-}}(6993)(2S)$	$\cdots$	3.16	3.45	2.65	0.54	$\cdots$/$\cdots$	$\cdots$
$T_{(4c)0^{+-}}(7020)(2S)$	$\cdots$	21.1	0.17	0.35	0.34	$\cdots$/$\cdots$	$\cdots$
$T_{(4c)1^{+-}}(6919)(2S)$	0.05	$\cdots$	0.02	0.04	0.06	0.09/0.68	$\cdots$
$T_{(4c)1^{+-}}(7021)(2S)$	1.98	$\cdots$	0.02	0.07	0.12	0.71/0.61	150
$T_{(4c)2^{+-}}(7017)(2S)$	$\cdots$	$\cdots$	4.70	3.75	0.86	$\cdots$/$\cdots$	$\cdots$
$T_{(4c)0^{--}}(6651)(1P)$	0.24	$\cdots$	0.00	6.75	$\cdots$	$\cdots$/$\cdots$	$\cdots$
$T_{(4c)0^{--}}(6926)(1P)$	0.12	$\cdots$	0.02	2.76	0.19	0.00/0.00	$\cdots$
$T_{(4c)1^{--}}(6636)(1P)$	0.04	0.02	3.28	0.97	$\cdots$	$\cdots$/$\cdots$	$\cdots$
$T_{(4c)1^{--}}(6750)(1P)$	0.17	0.01	1.92	3.99	1.05	0.00/0.00	$\cdots$
$T_{(4c)1^{--}}(6768)(1P)$	0.00	2.77	0.08	0.99	0.79	0.00/0.00	$\cdots$
$T_{(4c)1^{--}}(6904)(1P)$	0.00	0.17	2.96	0.26	0.17	0.00/0.00	$\cdots$
$T_{(4c)1^{--}}(6993)(1P)$	0.03	1.91	0.12	0.76	1.49	0.00/0.00	0.17
$T_{(4c)2^{--}}(6630)(1P)$	0.06	0.01	0.01	0.02	$\cdots$	$\cdots$/$\cdots$	$\cdots$
$T_{(4c)2^{--}}(6780)(1P)$	0.01	0.01	0.01	3.55	2.00	0.00/0.00	$\cdots$
$T_{(4c)2^{--}}(6955)(1P)$	0.00	0.00	0.11	1.75	3.45	0.00/0.01	0.00
$T_{(4c)3^{--}}(6801)(1P)$	0.00	0.00	0.16	0.27	11.8	0.00/0.00	$\cdots$

TABLE III. Fall-apart decay properties for the $T_{(4b)}$ states. The unit of the partial widths of each channel is MeV.

State	$\eta_b\eta_b$	$\Upsilon\Upsilon$	$\eta_b\eta_b(2S)$	$\Upsilon\Upsilon(2S)$	$\chi_{b0}\chi_{b0}/\chi_{b0}\chi_{b1}$	$\chi_{b0}\chi_{b2}/\chi_{b1}\chi_{b1}$	$\chi_{b1}\chi_{b2}/\chi_{b2}\chi_{b2}/h_bh_b$
$T_{(4b)0^{++}}(19306)(1S)$	0.33	0.16	$\cdots$	$\cdots$	$\cdots$	$\cdots$	$\cdots$
$T_{(4b)0^{++}}(19355)(1S)$	0.02	0.38	$\cdots$	$\cdots$	$\cdots$	$\cdots$	$\cdots$
$T_{(4b)2^{++}}(19341)(1S)$	$\cdots$	0.00	$\cdots$	$\cdots$	$\cdots$	$\cdots$	$\cdots$
$T_{(4b)0^{++}}(19719)(2S)$	0.11	0.21	1.04	1.53	$0.20/\cdots$	$\cdots$	$\cdots$
$T_{(4b)0^{++}}(19767)(2S)$	0.09	2.29	1.00	15.4	$14.2/\cdots$	$\cdots$	$\cdots$
$T_{(4b)0^{++}}(19811)(2S)$	3.80	1.89	24.0	8.30	$5.58/\cdots$	$0.01/18.2$	$0.66/\cdots/233$
$T_{(4b)0^{++}}(19976)(2S)$	0.07	0.69	0.32	2.02	$1.18/\cdots$	$0.09/4.27$	$0.67/10.4/5.50$
$T_{(4b)2^{++}}(19726)(2S)$	$\cdots$	0.41	$\cdots$	3.23	0.00	$\cdots$	$\cdots$
$T_{(4b)2^{++}}(19816)(2S)$	$\cdots$	7.41	$\cdots$	41.8	$0.03/15.2$	$45.3/34.5$	$75.8/\cdots/\cdots$

State	$\Upsilon\Upsilon$	$\eta_b\chi_{b0}$	$\eta_b\chi_{b1}$	$\eta_b\chi_{b2}$	Υh_b	$\Upsilon\Upsilon(2S)/\eta_b\eta_b(2S)$	$\chi_{b0}\chi_{b0}/\chi_{b0}\chi_{b1}/\chi_{b0}\chi_{b2}$
$T_{(4b)1^{++}}(19792)(2S)$	$\cdots$	5.41	16.3	23.9	58.0	$0.00/\cdots$	$\cdots/0.00/0.00$
$T_{(4b)0^{-+}}(19500)(1P)$	0.05	1.96	0.00	0.10	1.48	$0.00/\cdots$	$\cdots$
$T_{(4b)0^{-+}}(19595)(1P)$	0.16	1.26	0.00	0.15	3.74	$0.00/\cdots$	$\cdots$
$T_{(4b)0^{-+}}(19739)(1P)$	0.01	0.99	0.00	0.27	0.07	$0.00/\cdots$	$0.00/\cdots/\cdots$
$T_{(4b)1^{-+}}(19496)(1P)$	0.02	0.00	2.00	0.07	1.94	$0.00/0.00$	$\cdots$
$T_{(4b)1^{-+}}(19603)(1P)$	0.03	0.00	2.14	0.16	3.75	$0.00/0.00$	$\cdots$
$T_{(4b)1^{-+}}(19748)(1P)$	0.00	0.00	0.59	0.05	0.25	$0.00/0.00$	$0.07/\cdots/\cdots$
$T_{(4b)2^{-+}}(19492)(1P)$	0.00	0.00	0.01	0.03	0.03	$0.00/\cdots$	$\cdots$
$T_{(4b)2^{-+}}(19609)(1P)$	0.00	0.04	0.08	1.17	1.66	$0.00/\cdots$	$\cdots$
$T_{(4b)2^{-+}}(19756)(1P)$	0.00	0.06	0.11	1.01	1.58	$0.00/\cdots$	$0.00/\cdots/\cdots$

state	$\eta_b\Upsilon$	$\eta_b h_b$	$\chi_{b0}\Upsilon$	$\chi_{b1}\Upsilon$	$\chi_{b2}\Upsilon$	$\eta_b\Upsilon(2S)/\eta_b(2S)\Upsilon$	$\chi_{b0}h_b$
$T_{(4b)1^{+-}}(19329)(1S)$	0.10	$\cdots$	$\cdots$	$\cdots$	$\cdots$	$\cdots$	$\cdots$
$T_{(4b)0^{+-}}(19789)(2S)$	$\cdots$	66.8	4.10	12.0	17.3	$\cdots$	$\cdots$
$T_{(4b)0^{+-}}(19841)(2S)$	$\cdots$	15.9	3.42	10.5	16.0	$\cdots$	$\cdots$
$T_{(4b)1^{+-}}(19722)(2S)$	0.20	$\cdots$	0.00	0.01	0.01	$267/303$	$\cdots$
$T_{(4b)1^{+-}}(19813)(2S)$	1.82	$\cdots$	0.00	0.01	0.01	$82.7/102$	27
$T_{(4b)2^{+-}}(19795)(2S)$	$\cdots$	$\cdots$	12.6	37.0	54.0	$\cdots$	$\cdots$
$T_{(4b)0^{--}}(19485)(1P)$	0.04	$\cdots$	0.00	5.07	0.05	$0.00/0.00$	$\cdots$
$T_{(4b)0^{--}}(19756)(1P)$	0.02	$\cdots$	0.00	0.98	0.11	$0.00/0.00$	$\cdots$
$T_{(4b)1^{--}}(19479)(1P)$	0.01	0.00	2.01	1.09	1.90	$0.00/0.00$	$\cdots$
$T_{(4b)1^{--}}(19597)(1P)$	0.02	0.09	3.00	2.49	0.68	$0.00/0.00$	$\cdots$
$T_{(4b)1^{--}}(19603)(1P)$	0.00	3.65	0.03	0.91	0.67	$0.00/0.00$	$\cdots$
$T_{(4b)1^{--}}(19748)(1P)$	0.00	0.02	0.89	0.21	0.13	$0.00/0.00$	$\cdots$
$T_{(4b)1^{--}}(19795)(1P)$	0.00	0.99	0.14	0.55	0.54	$0.00/0.00$	0.04
$T_{(4b)2^{--}}(19476)(1P)$	0.01	0.00	0.00	0.01	0.06	$0.00/0.00$	$\cdots$
$T_{(4b)2^{--}}(19608)(1P)$	0.00	0.00	0.01	2.52	1.16	$0.00/0.00$	$\cdots$
$T_{(4b)2^{--}}(19767)(1P)$	0.00	0.00	0.09	1.08	2.17	$0.00/0.00$	0.00
$T_{(4b)3^{--}}(19617)(1P)$	0.00	0.00	0.15	0.30	6.85	$0.00/0.00$	$\cdots$

and ∼19.5–19.8 GeV, respectively. The masses of some 1P-wave $T_{(4c)}$ states are comparable with the newly observed structures $X(6600)$ and $X(6900)$.

It should be mentioned that except for the color configurations $|6\bar{6}\rangle_c$ and $|\bar{3}3\rangle_c$, one can also select the $|11\rangle_c$ and $|88\rangle_c$ representations when constructing the tetraquark wave functions. The two sets of color configurations are equivalent to each other. The $|6\bar{6}\rangle_c$ and $|\bar{3}3\rangle_c$ configurations

can be expressed by $|11\rangle_c$ and $|88\rangle_c$ through the Fierz transformation [35], with which one can extract the $|11\rangle_c$ and $|88\rangle_c$ components in physical states expressed with the $|6\bar{6}\rangle_c$ and $|\bar{3}3\rangle_c$ configurations. The components of different color configurations for the physical $T_{(4c)}$ and $T_{(4b)}$ states are given in the Tables VI and VII of the Appendix. To know the spatial size of the tetraquark states, we also calculate the root mean square radius, our results are also

listed in Tables VI and VII. Similar to ours, a systematical study of the 1S, 2S, and 1P-wave $T_{(4c)}$ states was also carried out within the nonrelativistic quark model in Ref. [57]. The obtained results are generally consistent with ours. The slight differences are mainly due to the different selections of the model parameters, spin-orbital potentials, and numerical methods. The differences of the numerical methods adopted in the present work and that in Ref. [57] have been discussed in Ref. [35].

In addition to calculating the mass spectra, the results of the fall-apart decays via the quark rearrangement of the 1S-, 2S-, and 1P-wave $T_{(4Q)}$ states are also given in Tables II and III. To our surprise, the fall-apart decay widths for most of the $T_{(4Q)}$ states are only in a small range of ~0–10 MeV. Thus, there should exist some stable $T_{(4Q)}$ states although their masses are above the thresholds of $Q\bar{Q}$ meson pairs.

In the following part, we focus on the 1S-, 2S-, and 1P-wave $T_{(4c)}$ states to understand the di-J/ψ spectrum observed at LHCb [38], CMS [40], and ATLAS [39]. The nature of the broad structure around 6.2–6.8 GeV in the di-J/ψ invariant mass spectrum [38–40] is mysterious if it is a genuine state since it is difficult to understand what decay channels would contribute to its broad width. Note that the CMS [40] and ATLAS [39] measurements show some details where a small shoulder appears at the lower side of the broad structure $X(6600)$.

There are no $T_{(4c)}$ states lying in the mass range of <6.4 GeV in our NRPQM predictions. However, it turns out to be possible that the small-shoulder structure around 6.2–6.4 GeV near the di-J/ψ threshold may be caused by some feed-down effects from higher mass $T_{(4c)}$ states. It is interesting to find that in the 2S-wave $T_{(4c)}$ states, the quark rearrangement decay rates of $T_{(4c)0^{++}}(6908, 6957, 7018) \rightarrow \chi_{c0}\chi_{c0}$, $T_{(4c)0^{++}}(7185) \rightarrow \chi_{c1}\chi_{c1}, \chi_{c2}\chi_{c2}$ are large, and their partial widths are predicted to be $\mathcal{O}(10)$ MeV. These 2S-wave states with $J^{PC} = 0^{++}$ have masses around ~6.9–7.2 GeV. The $\chi_{cJ}\chi_{cJ'}$ final states can feed down to the di-J/ψ channel via $\chi_{cJ}\chi_{cJ'} \rightarrow J/\psi J/\psi + \gamma\gamma$ and $J/\psi J/\psi + \pi\pi$ where the two soft photons or soft pions will evade the detection.

We actually find that there could be multi-sources contributing to the shoulder structure around 6.2–6.4 GeV via the feed-down mechanisms from some 1P-wave $T_{(4c)}$ states. For instance, the decay rates for $T_{(4c)0^{--}}(6651) \rightarrow J/\psi\chi_{c1}$, $T_{(4c)1^{--}}(6636) \rightarrow J/\psi\chi_{c0}$, $T_{(4c)1^{--}}(6750) \rightarrow J/\psi\chi_{c0,1,2}$, $T_{(4c)2^{--}}(6780) \rightarrow J/\psi\chi_{c1,2}$, and $T_{(c c\bar{c}\bar{c})3^{--}}(6801) \rightarrow J/\psi\chi_{c2}$ are quite large. Their partial widths are predicted to be about several MeV. These 1P-wave states have masses in the range of ~6.6–6.8 GeV. Their decays into $J/\psi\chi_{cJ}$ can also contribute to the di-J/ψ channel through the radiative decays of $J/\psi\chi_{c0,1,2} \rightarrow J/\psi J/\psi\gamma$, where the photon momenta are about 300–450 MeV. The feed-down mechanism seems to

be a possible explanation for the broad structure around 6.2–6.4 GeV in the di-J/ψ invariant mass spectrum.

The $X(6600)$ structure observed at CMS may be assigned to the 1S-wave state $T_{(4c)0^{++}}(6550)$ predicted in the NRPQM. This state is a mixed state between two color configurations $6\bar{6}$ and $\bar{3}3$. The predicted mass is in good agreement with the observations. Furthermore, the quark rearrangement decays of $T_{(4c)0^{++}}(6550)$ are governed by the di-J/ψ channel, which is also consistent with the observations. Although the predicted partial width of the di-J/ψ mode, $\Gamma_{J/\psi J/\psi} \simeq 1.78$ MeV, is much smaller than the observed total width $\Gamma = 124 \pm 29 \pm 34$ MeV of $X(6600)$, its width may be saturated by the hadronic decays into open-charmed meson pairs via the $c\bar{c}$ annihilations [18]. It was shown in Ref. [18] that the sum of the partial widths of these hadronic decay processes can reach up to order of 100 MeV. In the same picture the other 1S state $T_{(4c)0^{++}}(6455)$ may also be observed in the di-J/ψ channel given the accumulation of more data in the future. Finally, it should be mentioned that the $X(6600)$ structure may also bear some feed-down effects from the 2S-wave states $T_{(4c)0^{+-}}(6978)$ and $T_{(4c)2^{+-}}(7031)$, and/or the 1P-wave states $T_{(4c)0^{--}}(6926)$, $T_{(4c)1^{--}}(6904, 6993)$ and $T_{(4c)2^{--}}(6955)$, since they have sizeable partial widths into $J/\psi\chi_{cJ}$ final states.

Concerning the nature of $X(6900)$ the mass location suggests that several 1P- and 2S-wave states with $C = +1$ can be the candidates of $X(6900)$. However, with the decay properties taken into account it shows that only the 2S-wave state $T_{(4c)0^{++}}(6957)$ can match $X(6900)$. The partial widths of $T_{(4c)0^{++}}(6957)$ decaying into the di-J/ψ and $J/\psi\psi(2S)$ channels are predicted to be ~4.7 MeV and 3.2 MeV, respectively. Combined with the measured width $\Gamma = 122 \pm 22 \pm 19$ MeV of $X(6900)$, it is predicted that the decay rates of these two channels are $\mathcal{O}(3\%)$. As listed in Table I, $T_{(4c)0^{++}}(6957)$ contains dominantly $2^1S_{0^{++}(6\bar{6})_c}(\xi_1,\xi_2)$. Its mass slightly higher than $T_{(4c)0^{++}}(6908)$ of which the dominant configuration is $2^1S_{0^{++}(\bar{3}3)_c}(\xi_3)$. This is due to the strong attraction produced by the relatively small but crucial mixing of the $2^1S_{0^{++}(\bar{3}3)_c}(\xi_3)$ configuration. Its crucial role for the $2^1S_{0^{++}}$ multiplets can be seen clearly by the mixing matrix in Table I for both $cc\bar{c}\bar{c}$ and $bb\bar{b}\bar{b}$.

With $X(6900)$ assigned as the $T_{(4c)0^{++}}(6957)$, the partial width ratio between the di-J/ψ and $J/\psi\psi(2S)$ channels is predicted to be

$$\frac{\Gamma_{J/\psi J/\psi}}{\Gamma_{J/\psi\psi(2S)}} \simeq 1.5, \tag{8}$$

which can be tested in future experiments. As shown in Table II, the main decay channel of $T_{(4c)0^{++}}(6957)$ should be $T_{(4c)0^{++}}(6957) \rightarrow \chi_{c0}\chi_{c0}$. Therefore, a search for $X(6900)$ in the $\chi_{c0}\chi_{c0}$ channel could be useful for

understanding its nature. We notice that some other analyses also prefer $X(6900)$ as a compact tetraquark state with $J^{PC} = 0^{++}$ [73,91,92]. Finally, it should be mentioned that the $2S$ state $T_{(4c)0^{++}}(7018)$ may also contribute to the $X(6900)$ structure observed in the di-J/ψ final state, since it has a sizeable partial decay width, $\Gamma_{J/\psi J/\psi} \simeq 1.87$ MeV, into the di-J/ψ channel. Moreover, this state has large decay rates into the $\eta_c \eta_c$ and $\chi_{c0} \chi_{c0}$ channels as well.

IV. SUMMARY

With the coherent study of the fully-heavy tetraquark spectra in the NRPQM and their rearrangement decays, we show that the recent measurements of the di-J/ψ spectrum have provided a strong evidence for the S- and P-wave $T_{(4c)}$ states. The small shoulder structure around 6.2–6.4 GeV observed by CMS and ATLAS may be due to the feed-down effects from higher $1P$-wave states with $C = -1$ or some $2S$-wave states with $J^{PC} = 0^{++}$. The $X(6600)$ structure may arise from the $1S$-wave state $T_{(4c)0^{++}}(6550)$, of which the peak structure may also bear some feed-down effects from the $2S$-wave and/or $1P$-wave states with $C = -1$. The $X(6900)$ structure is most likely to be the $2S$-wave state $T_{(4c)0^{++}}(6957)$. If $X(6600)$ and $X(6900)$ indeed correspond to the $1S$- and $2S$-wave $T_{(4c)}$ states, respectively, their decay rates into the di-J/ψ channel are predicted to be order of 1%. In addition, one $1S$-state $T_{(4c)0^{++}}(6455)$, one $2S$-state $T_{(4c)0^{++}}(7016)$ and one $1P$-state $T_{(4c)0^{-+}}(6749)$ are predicted to be located at the same masses as $X(6600)$ and $X(6900)$ in the di-J/ψ invariant mass spectrum.

Based on such a scenario, we expect that more signals for the $T_{(4c)}$ states should be observed in other decay channels via either S- or P-wave transitions, such as $\eta_c \eta_c$, $J/\psi h_c$, $J/\psi \chi_{cJ}$, and $\eta_c h_c$. By extending the calculations to the full-bottom tetraquark systems, we have also included the mass spectra of the $bb\bar{b}\bar{b}$ states and their fall-apart decays in Table I and Table III, respectively. Several $2S$-wave $T_{(4b)}$ states, such as $T_{(4b)0^{++}}(19767)$ and $T_{(4b)0^{++}}(19811)$, should have good potentials to be observed in di-Υ and $\Upsilon\Upsilon(2S)$ decay channels. Notice that no signals of the $T_{(4b)}$ states are found based on the present statistics at LHCb [38]. This can be due to the low production rates for such heavy objects.

APPENDIX

The calculation of the decay amplitude $\mathcal{M}(A \to BC)$ of a $T_{(4Q)}$ state is indeed a tedious task. For simplicity, the spatial wave functions for the A, B, C hadron states are adopted a harmonic oscillator form, the harmonic oscillator parameters are determined by fitting the wave functions calculated from the potential model. These parameters have been given in Table IV and Table V.

Taking $T_{(cc\bar{c}\bar{c})0^{++}}(1S)(6455) \to J/\psi J/\psi$ as an example, from Table I one can obtain the wave function for the initial $T_{(cc\bar{c}\bar{c})0^{++}}(1S)(6455)$ state, i.e.,

$$|A\rangle = 0.58\psi_{000}^{1S}\chi_{00}^{00}|6\bar{6}\rangle_c + 0.81\psi_{000}^{1S}\chi_{00}^{11}|\bar{3}3\rangle_c, \quad (A1)$$

which is an admixture between several different configurations. The wave function of the final state is obtained within the $J - J$ coupling scheme. Combining with the Clebsch-Gordan coefficients, the wave function of the di-J/ψ system with quantum numbers $J^{PC} = 0^{++}$ is given by

$$|BC\rangle = \frac{1}{\sqrt{3}} [\chi_{11}^1 \chi_{1-1}^2 - \chi_{10}^1 \chi_{10}^2 + \chi_{1-1}^1 \chi_{11}^2]$$
$$\varphi_{000}^1 \varphi_{000}^2 \phi |11\rangle, \quad (A2)$$

where the superscripts 1,2 stand for the two J/ψ mesons in the final state, χ stands for the their spin wave functions, and φ_{000} stands for their spatial wave functions. ϕ is the wave function for describing the relative motion of two final-state mesons, which is adopted a plane wave form by treating the final state mesons as free particles,

$$\phi = \frac{1}{(2\pi\hbar)^{\frac{3}{2}}} e^{-i\boldsymbol{p}_f \cdot (\boldsymbol{r}_{f_1} - \boldsymbol{r}_{f_2})}, \quad (A3)$$

where $\boldsymbol{p}_f$ is the three-momentum of the hadron 1 in the final state, $\boldsymbol{r}_{f_1}$ and $\boldsymbol{r}_{f_2}$ stand for the position coordinates of the hadrons 1,2 in the final state.

TABLE IV. The masses (MeV) and harmonic oscillator parameters β (MeV) for the meson states.

State	$c\bar{c}$	Mass	β	$b\bar{b}$	Mass	β
1^1S_0	η_c	2984	658	η_b	9378	1160
1^3S_1	J/ψ	3097	564	Υ	9436	1096
2^1S_0	$\eta_c(2S)$	3635	506	$\eta_b(2S)$	9973	858
2^3S_1	$\psi(2S)$	3679	470	$\Upsilon(2S)$	9989	822
1^3P_0	χ_{c0}	3417	533	χ_{b0}	9845	822
1^1P_1	h_c	3522	459	h_b	9899	731
1^3P_1	χ_{c1}	3516	459	χ_{b1}	9891	759
1^3P_2	χ_{c2}	3552	429	χ_{b2}	9914	705

TABLE V.   The harmonic oscillator parameters β (MeV) for the $T_{(4Q)}$ state.

State	β	State	β	State	β	State	β
$T_{(c\bar{c}\bar{c})0^{++}}(1S)(6455)$	481	$T_{(c\bar{c}\bar{c})1^{+-}}(1S)(6500)$	493	$T_{(b\bar{b}\bar{b})0^{++}}(1S)(19306)$	897	$T_{(b\bar{b}\bar{b})1^{+-}}(1S)(19329)$	897
$T_{(c\bar{c}\bar{c})0^{++}}(1S)(6550)$	493	$T_{(c\bar{c}\bar{c})2^{++}}(1S)(6524)$	481	$T_{(b\bar{b}\bar{b})0^{++}}(1S)(19355)$	897	$T_{(b\bar{b}\bar{b})2^{++}}(1S)(19341)$	897
$T_{(c\bar{c}\bar{c})0^{+-}}(2S)(6993)$	403	$T_{(c\bar{c}\bar{c})1^{+-}}(2S)(6919)$	420	$T_{(b\bar{b}\bar{b})0^{+-}}(2S)(19789)$	680	$T_{(b\bar{b}\bar{b})1^{+-}}(2S)(19722)$	704
$T_{(c\bar{c}\bar{c})0^{+-}}(2S)(7020)$	420	$T_{(c\bar{c}\bar{c})1^{+-}}(2S)(7021)$	411	$T_{(b\bar{b}\bar{b})0^{+-}}(2S)(19841)$	704	$T_{(b\bar{b}\bar{b})1^{+-}}(2S)(19813)$	704
$T_{(c\bar{c}\bar{c})0^{++}}(2S)(6908)$	411	$T_{(c\bar{c}\bar{c})1^{++}}(2S)(7009)$	420	$T_{(b\bar{b}\bar{b})0^{++}}(2S)(19719)$	704	$T_{(b\bar{b}\bar{b})1^{++}}(2S)(19792)$	704
$T_{(c\bar{c}\bar{c})0^{++}}(2S)(6957)$	420	$T_{(c\bar{c}\bar{c})2^{+-}}(2S)(7017)$	411	$T_{(b\bar{b}\bar{b})0^{++}}(2S)(19767)$	730	$T_{(b\bar{b}\bar{b})2^{++}}(2S)(19795)$	704
$T_{(c\bar{c}\bar{c})0^{++}}(2S)(7018)$	420	$T_{(c\bar{c}\bar{c})2^{++}}(2S)(6927)$	411	$T_{(b\bar{b}\bar{b})0^{++}}(2S)(19811)$	704	$T_{(b\bar{b}\bar{b})2^{++}}(2S)(19726)$	704
$T_{(c\bar{c}\bar{c})0^{++}}(2S)(7185)$	411	$T_{(c\bar{c}\bar{c})2^{++}}(2S)(7032)$	411	$T_{(b\bar{b}\bar{b})0^{++}}(2S)(19976)$	704	$T_{(b\bar{b}\bar{b})2^{++}}(2S)(19816)$	704
$T_{(c\bar{c}\bar{c})0^{--}}(1P)(6651)$	438	$T_{(c\bar{c}\bar{c})1^{--}}(1P)(6904)$	438	$T_{(b\bar{b}\bar{b})0^{--}}(1P)(19485)$	789	$T_{(b\bar{b}\bar{b})1^{--}}(1P)(19748)$	789
$T_{(c\bar{c}\bar{c})0^{--}}(1P)(6926)$	438	$T_{(c\bar{c}\bar{c})1^{--}}(1P)(6993)$	438	$T_{(b\bar{b}\bar{b})0^{--}}(1P)(19756)$	759	$T_{(b\bar{b}\bar{b})1^{--}}(1P)(19795)$	759
$T_{(c\bar{c}\bar{c})0^{-+}}(1P)(6676)$	438	$T_{(c\bar{c}\bar{c})1^{-+}}(1P)(6675)$	438	$T_{(b\bar{b}\bar{b})0^{-+}}(1P)(19500)$	789	$T_{(b\bar{b}\bar{b})1^{-+}}(1P)(19496)$	789
$T_{(c\bar{c}\bar{c})0^{-+}}(1P)(6748)$	438	$T_{(c\bar{c}\bar{c})1^{-+}}(1P)(6768)$	438	$T_{(b\bar{b}\bar{b})0^{-+}}(1P)(19595)$	759	$T_{(b\bar{b}\bar{b})1^{-+}}(1P)(19603)$	759
$T_{(c\bar{c}\bar{c})0^{-+}}(1P)(6897)$	438	$T_{(c\bar{c}\bar{c})1^{-+}}(1P)(6910)$	438	$T_{(b\bar{b}\bar{b})0^{-+}}(1P)(19739)$	789	$T_{(b\bar{b}\bar{b})1^{-+}}(1P)(19748)$	789
$T_{(c\bar{c}\bar{c})1^{--}}(1P)(6636)$	438	$T_{(c\bar{c}\bar{c})2^{--}}(1P)(6630)$	438	$T_{(b\bar{b}\bar{b})1^{--}}(1P)(19479)$	789	$T_{(b\bar{b}\bar{b})2^{--}}(1P)(19476)$	789
$T_{(c\bar{c}\bar{c})1^{--}}(1P)(6750)$	438	$T_{(c\bar{c}\bar{c})2^{--}}(1P)(6780)$	438	$T_{(b\bar{b}\bar{b})1^{--}}(1P)(19597)$	759	$T_{(b\bar{b}\bar{b})2^{--}}(1P)(19608)$	759
$T_{(c\bar{c}\bar{c})1^{--}}(1P)(6768)$	438	$T_{(c\bar{c}\bar{c})2^{--}}(1P)(6955)$	438	$T_{(b\bar{b}\bar{b})1^{--}}(1P)(19603)$	759	$T_{(b\bar{b}\bar{b})2^{--}}(1P)(19767)$	759
$T_{(c\bar{c}\bar{c})2^{-+}}(1P)(6667)$	438	$T_{(c\bar{c}\bar{c})2^{-+}}(1P)(6783)$	438	$T_{(b\bar{b}\bar{b})2^{-+}}(1P)(19492)$	789	$T_{(b\bar{b}\bar{b})2^{-+}}(1P)(19609)$	759
$T_{(c\bar{c}\bar{c})2^{-+}}(1P)(6928)$	438	$T_{(c\bar{c}\bar{c})3^{--}}(1P)(6801)$	438	$T_{(b\bar{b}\bar{b})2^{-+}}(1P)(19756)$	789	$T_{(b\bar{b}\bar{b})3^{--}}(1P)(19617)$	759

By using the wave functions given in Eqs. (A1) and (A2), one can calculate the transition matrix element with

$$\langle BC|V_{ij}|A\rangle = \left(\left\langle \frac{1}{\sqrt{3}}[\chi^1_{11}\chi^2_{1-1} - \chi^1_{10}\chi^2_{10} + \chi^1_{1-1}\chi^2_{11}][11]_c\right|\right.$$
$$\left.\hat{O}^{sc}_{ij}|c_1\chi^{00}_{00}[6\bar{6}] + c_2\chi^{11}_{00}[\bar{3}3]_c\right\rangle\right)$$
$$\langle \varphi^1_{000}\varphi^2_{000}\phi|\hat{O}^o_{ij}|\psi^{1S}_{000}\rangle, \tag{A4}$$

where the $\hat{O}^{sc}_{ij}$ and $\hat{O}^o_{ij}$ stand for the spin-color dependent and spatial dependent operator, respectively. Calculating the matrix elements in color and spin space is relatively simple. When calculating the matrix element of the spatial part, $\langle\varphi^1_{000}\varphi^2_{000}\phi|\hat{O}^o_{ij}|\psi^{1S}_{000}\rangle$, one should face a problem. The spatial wave function, which contains three different variables, cannot be separated into the product of three functions with independent variables directly. One should solve this problem by defining new coordinate systems via

TABLE VI.   The components of different color configurations and the root mean square radii (fm) for each physical $T_{(4c)}$ states, where $\boldsymbol{r}_{12-34} \equiv (\boldsymbol{r}_1 + \boldsymbol{r}_2)/2 - (\boldsymbol{r}_3 + \boldsymbol{r}_4)/2$, $\boldsymbol{r}_{13-24} \equiv (\boldsymbol{r}_1 + \boldsymbol{r}_3)/2 - (\boldsymbol{r}_2 + \boldsymbol{r}_4)/2$.

State	$|6\bar{6}\rangle_c$	$|\bar{3}3\rangle_c$	$|11\rangle_c$	$|88\rangle_c$	$\sqrt{\langle r^2_{12}\rangle}$	$\sqrt{\langle r^2_{12-34}\rangle}$	$\sqrt{\langle r^2_{13}\rangle}$	$\sqrt{\langle r^2_{13-24}\rangle}$
$T_{(4c)0^{++}}(6455)(1S)$	33.9%	66.1%	44.6%	55.4%	0.49	0.35	0.49	0.35
$T_{(4c)0^{++}}(6550)(1S)$	66.1%	33.9%	55.4%	44.6%	0.50	0.35	0.50	0.35
$T_{(4c)1^{+-}}(6500)(1S)$	0.0%	100.0%	33.3%	66.7%	0.50	0.35	0.50	0.35
$T_{(4c)2^{++}}(6524)(1S)$	0.0%	100.0%	33.3%	66.7%	0.51	0.36	0.51	0.36
$T_{(4c)0^{--}}(6651)(1P)$	64.0%	36.0%	54.7%	45.3%	0.63	0.39	0.59	0.45
$T_{(4c)0^{--}}(6926)(1P)$	36.0%	64.0%	45.3%	54.7%	0.63	0.39	0.59	0.45
$T_{(4c)0^{-+}}(6681)(1P)$	67.5%	32.5%	55.8%	44.2%	0.61	0.39	0.59	0.43
$T_{(4c)0^{-+}}(6749)(1P)$	2.0%	98.0%	34.0%	66.0%	0.55	0.47	0.61	0.39
$T_{(4c)0^{-+}}(6891)(1P)$	30.1%	69.9%	43.4%	56.6%	0.62	0.39	0.59	0.44
$T_{(4c)1^{--}}(6636)(1P)$	67.8%	32.2%	55.9%	44.1%	0.63	0.39	0.59	0.44
$T_{(4c)1^{--}}(6750)(1P)$	0.4%	99.6%	33.5%	66.5%	0.54	0.48	0.61	0.38
$T_{(4c)1^{--}}(6768)(1P)$	1.0%	99.0%	33.7%	663%.	0.55	0.50	0.63	0.39
$T_{(4c)1^{--}}(6904)(1P)$	48.4%	51.6%	49.5%	50.5%	0.60	0.42	0.60	0.43
$T_{(4c)1^{--}}(6993)(1P)$	83.5%	16.5%	61.2%	38.8%	0.57	0.47	0.62	0.4

(Table continued)

TABLE VI. *(Continued)*

State	$\lvert 6\bar{6}\rangle_c$	$\lvert \bar{3}3\rangle_c$	$\lvert 11\rangle_c$	$\lvert 88\rangle_c$	$\sqrt{\langle r_{12}^2\rangle}$	$\sqrt{\langle r_{12-34}^2\rangle}$	$\sqrt{\langle r_{13}^2\rangle}$	$\sqrt{\langle r_{13-24}^2\rangle}$
$T_{(4c)1^{-+}}(6676)(1P)$	68.0%	32.0%	56.0%	44.0%	0.63	0.39	0.59	0.45
$T_{(4c)1^{-+}}(6769)(1P)$	0.0%	100.0%	33.3%	66.7%	0.55	0.50	0.63	0.39
$T_{(4c)1^{-+}}(6908)(1P)$	32.5%	67.5%	44.2%	55.8%	0.62	0.38	0.59	0.44
$T_{(4c)2^{--}}(6630)(1P)$	64.5%	35.5%	54.8%	45.2%	0.64	0.39	0.60	0.45
$T_{(4c)2^{--}}(6780)(1P)$	0.0%	100.0%	33.3%	66.7%	0.55	0.50	0.63	0.39
$T_{(4c)2^{--}}(6955)(1P)$	35.6%	64.4%	45.2%	54.8%	0.63	0.39	0.59	0.45
$T_{(4c)2^{-+}}(6667)(1P)$	67.2%	32.8%	55.7%	44.3%	0.63	0.39	0.59	0.45
$T_{(4c)2^{-+}}(6783)(1P)$	0.0%	100.0%	33.3%	66.7%	0.55	0.50	0.64	0.39
$T_{(4c)2^{-+}}(6928)(1P)$	33.7%	66.3%	44.6%	55.4%	0.63	0.39	0.59	0.45
$T_{(4c)3^{--}}(6801)(1P)$	0.0%	100.0%	33.3%	66.7%	0.56	0.51	0.64	0.39
$T_{(4c)0^{+-}}(6993)(2S)$	43.6%	56.4%	47.9%	52.1%	0.77	0.43	0.69	0.54
$T_{(4c)0^{+-}}(7020)(2S)$	56.4%	43.6%	52.1%	47.9%	0.78	0.42	0.69	0.55
$T_{(4c)0^{++}}(6908)(2S)$	12.5%	87.5%	37.5%	62.5%	0.45	0.66	0.73	0.32
$T_{(4c)0^{++}}(6957)(2S)$	83.0%	17.0%	61.0%	39.0%	0.76	0.42	0.69	0.54
$T_{(4c)0^{++}}(7018)(2S)$	4.4%	95.6%	34.8%	65.2%	0.56	0.56	0.69	0.40
$T_{(4c)0^{++}}(7185)(2S)$	99.7%	0.3%	66.6%	33.4%	0.74	0.33	0.62	0.52
$T_{(4c)1^{+-}}(6919)(2S)$	0.0%	100.0%	33.3%	66.7%	0.52	0.72	0.82	0.37
$T_{(4c)1^{+-}}(7021)(2S)$	0.0%	100.0%	33.3%	66.7%	0.69	0.36	0.61	0.49
$T_{(4c)1^{++}}(7009)(2S)$	0.0%	100.0%	33.3%	66.7%	0.73	0.45	0.68	0.51
$T_{(4c)2^{+-}}(7017)(2S)$	0.0%	100.0%	33.3%	66.7%	0.73	0.45	0.68	0.52
$T_{(4c)2^{++}}(6927)(2S)$	0.0%	100.0%	33.3%	66.7%	0.47	0.68	0.76	0.33
$T_{(4c)2^{++}}(7032)(2S)$	0.0%	100.0%	33.3%	66.7%	0.79	0.45	0.72	0.56

coordinate transformations by using the standard linear algebra methods [105,106].

Then, the integration of the spatial part is shown. It is given by

$$
\begin{aligned}
&\langle \varphi_{000}^1(\omega_{f_1})\varphi_{000}^2(\omega_{f_2})\phi\lvert \hat{O}_{ij}^o\lvert \psi_{000}^{1S}(\omega_i)\rangle \\
&= I_{\mathrm{Nor}}\int \hat{O}e^{-\sum_{i,j}A_{ij}\boldsymbol{\xi}_i\cdot\boldsymbol{\xi}_j}e^{-i\mathbf{p}_f\cdot\boldsymbol{\xi}_3}(Y_{00})^5 d^3\boldsymbol{\xi}_1 d^3\boldsymbol{\xi}_2 d^3\boldsymbol{\xi}_3,
\end{aligned}\quad (A5)
$$

where I_{Nor} is a normalization factor independent of the integration variable, and the matrix A is given by

$$
A = \begin{pmatrix}
\frac{1}{2}\mu\omega_i^2 + \frac{1}{4}\mu\omega_f^2 & -\frac{1}{4}\mu\omega_f^2 & 0 \\
-\frac{1}{4}\mu\omega_f^2 & \frac{1}{2}\mu\omega_i^2 + \frac{1}{4}\mu\omega_f^2 & 0 \\
0 & 0 & \mu\omega_i^2 + \mu\omega_f^2
\end{pmatrix}.
\quad (A6)
$$

TABLE VII. The components of different color configurations and the root mean square radii (fm) for each physical $T_{(4b)}$ states, where $r_{12-34} \equiv (\mathbf{r}_1 + \mathbf{r}_2)/2 - (\mathbf{r}_3 + \mathbf{r}_4)/2$, $r_{13-24} \equiv (\mathbf{r}_1 + \mathbf{r}_3)/2 - (\mathbf{r}_2 + \mathbf{r}_4)/2$.

State	$\lvert 6\bar{6}\rangle_c$	$\lvert \bar{3}3\rangle_c$	$\lvert 11\rangle_c$	$\lvert 88\rangle_c$	$\sqrt{\langle r_{12}^2\rangle}$	$\sqrt{\langle r_{12-34}^2\rangle}$	$\sqrt{\langle r_{13}^2\rangle}$	$\sqrt{\langle r_{13-24}^2\rangle}$
$T_{(4b)0^{++}}(19306)(1S)$	33.9%	66.1%	44.6%	55.4%	0.27	0.19	0.27	0.19
$T_{(4b)0^{++}}(19355)(1S)$	66.1%	33.9%	55.4%	44.6%	0.27	0.19	0.27	0.19
$T_{(4b)1^{+-}}(19329)(1S)$	0.0%	100.0%	33.3%	66.7%	0.27	0.19	0.27	0.19
$T_{(4b)2^{++}}(19341)(1S)$	0.0%	100.0%	33.3%	66.7%	0.27	0.19	0.27	0.19
$T_{(4b)0^{--}}(19485)(1P)$	65.3%	34.7%	55.1%	44.9%	0.36	0.22	0.34	0.25
$T_{(4b)0^{--}}(19756)(1P)$	34.7%	65.3%	44.9%	55.1%	0.36	0.22	0.34	0.26
$T_{(4b)0^{-+}}(19500)(1P)$	68.0%	32.0%	56.0%	44.0%	0.35	0.22	0.33	0.25
$T_{(4b)0^{-+}}(19595)(1P)$	0.0%	100.0%	33.3%	66.7%	0.31	0.28	0.36	0.22
$T_{(4b)0^{-+}}(19739)(1P)$	32.5%	67.5%	44.2%	55.8%	0.36	0.22	0.33	0.25
$T_{(4b)1^{--}}(19479)(1P)$	67.1%	32.9%	55.7%	44.3%	0.36	0.22	0.34	0.26

(Table continued)

TABLE VII. (Continued)

State	$\|6\bar{6}\rangle_c$	$\|\bar{3}3\rangle_c$	$\|11\rangle_c$	$\|88\rangle_c$	$\sqrt{\langle r_{12}^2\rangle}$	$\sqrt{\langle r_{12-34}^2\rangle}$	$\sqrt{\langle r_{13}^2\rangle}$	$\sqrt{\langle r_{13-24}^2\rangle}$
$T_{(4b)1^{--}}(19597)(1P)$	91.9%	8.1%	64.0%	36.0%	0.31	0.28	0.36	0.22
$T_{(4b)1^{--}}(19603)(1P)$	0.0%	100.0%	33.3%	66.7%	0.31	0.28	0.36	0.22
$T_{(4b)1^{--}}(19748)(1P)$	0.2%	99.8%	33.4%	66.6%	0.36	0.23	0.35	0.25
$T_{(4b)1^{--}}(19795)(1P)$	41.3%	58.7%	47.1%	52.9%	0.33	0.29	0.37	0.23
$T_{(4b)1^{-+}}(19496)(1P)$	67.3%	32.7%	55.8%	44.2%	0.36	0.22	0.34	0.25
$T_{(4b)1^{-+}}(19603)(1P)$	0.0%	100.0%	33.3%	66.7%	0.31	0.28	0.36	0.22
$T_{(4b)1^{-+}}(19748)(1P)$	32.5%	67.5%	44.2%	55.8%	0.36	0.22	0.34	0.26
$T_{(4b)2^{--}}(19476)(1P)$	65.3%	34.7%	55.1%	44.9%	0.36	0.22	0.34	0.25
$T_{(4b)2^{--}}(19608)(1P)$	0.0%	100.0%	33.3%	66.7%	0.31	0.29	0.36	0.22
$T_{(4b)2^{--}}(19767)(1P)$	34.6%	65.4%	44.9%	55.1%	0.36	0.22	0.34	0.26
$T_{(4b)2^{-+}}(19492)(1P)$	66.7%	33.3%	55.6%	44.4%	0.36	0.22	0.34	0.25
$T_{(4b)2^{-+}}(19609)(1P)$	0.0%	100.0%	33.3%	66.7%	0.31	0.29	0.36	0.22
$T_{(4b)2^{-+}}(19756)(1P)$	33.3%	66.7%	44.4%	55.6%	0.36	0.22	0.34	0.26
$T_{(4b)3^{--}}(19617)(1P)$	0.0%	100.0%	33.3%	66.7%	0.32	0.29	0.36	0.22
$T_{(4b)0^{+-}}(19789)(2S)$	1.0%	99.0%	33.7%	66.3%	0.43	0.28	0.42	0.31
$T_{(4b)0^{+-}}(19841)(2S)$	99.0%	1.0%	66.3%	33.7%	0.48	0.24	0.42	0.34
$T_{(4b)0^{++}}(19719)(2S)$	2.4%	97.6%	34.1%	65.9%	0.41	0.20	0.35	0.29
$T_{(4b)0^{++}}(19767)(2S)$	1.0%	99.0%	33.7%	66.3%	0.28	0.43	0.48	0.20
$T_{(4b)0^{++}}(19811)(2S)$	96.2%	3.8%	65.4%	34.6%	0.32	0.36	0.43	0.22
$T_{(4b)0^{++}}(19976)(2S)$	100.0%	0.0%	66.7%	33.3%	0.39	0.16	0.31	0.28
$T_{(4b)1^{+-}}(19722)(2S)$	0.0%	100.0%	33.3%	66.7%	0.40	0.20	0.35	0.28
$T_{(4b)1^{+-}}(19813)(2S)$	0.0%	100.0%	33.3%	66.7%	0.30	0.44	0.49	0.21
$T_{(4b)1^{++}}(19792)(2S)$	0.0%	100.0%	33.3%	66.7%	0.43	0.28	0.41	0.30
$T_{(4b)2^{+-}}(19795)(2S)$	0.0%	100.0%	33.3%	66.7%	0.43	0.28	0.42	0.31
$T_{(4b)2^{++}}(19726)(2S)$	0.0%	100.0%	33.3%	66.7%	0.38	0.20	0.34	0.27
$T_{(4b)2^{++}}(19816)(2S)$	0.0%	100.0%	33.3%	66.7%	0.31	0.43	0.49	0.22

Note that $A_{23} = 0$, the matrix A can be transformed into a diagonal matrix,

$$A' = \begin{pmatrix} A_{11} - \frac{A_{12}^2}{A_{22}} & 0 & 0 \\ 0 & A_{22} & 0 \\ 0 & 0 & A_{33} \end{pmatrix}, \quad \text{(A7)}$$

through the coordinate transformations, $\boldsymbol{\xi}_1' = \boldsymbol{\xi}_1$, $\boldsymbol{\xi}_2' = \frac{-A_{12}'}{A_{22}'}\boldsymbol{\xi}_1 + \frac{-A_{12}'}{A_{22}'}\boldsymbol{\xi}_2$, $\boldsymbol{\xi}_3' = \boldsymbol{\xi}_3$. On the other hand, in the calculations, the plane wave should be expanded by

$$e^{i\boldsymbol{P}\cdot\boldsymbol{r}} = \sum_{l=0}^{\infty}\sqrt{4\pi(2l+1)}i^l j_l(Pr)Y_{l0}(\hat{\boldsymbol{r}}), \quad \text{(A8)}$$

where we let the momentum P along the z direction. With the above steps, one can obtain the integration of the spatial part.

The components of different color configurations for the physical $T_{(4c)}$ and $T_{(4b)}$ states are given in the Tables VI and VII, respectively. To know the spatial size of the tetraquark states, we also calculate the root mean square radius, our results are listed in Tables VI and VII as well.

[1] M. Gell-Mann, A schematic model of baryons and mesons, Phys. Lett. **8**, 214 (1964).

[2] G. Zweig, An SU(3) model for strong interaction symmetry and its breaking. Version 1, Report No. CERN-TH-401.

[3] S. K. Choi *et al.* (Belle Collaboration), Observation of a narrow charmonium - like state in exclusive $B^\pm \to K^\pm\pi^+\pi^- J/\psi$ decays, Phys. Rev. Lett. **91**, 262001 (2003).

[4] S. L. Olsen, T. Skwarnicki, and D. Zieminska, Nonstandard heavy mesons and baryons: Experimental evidence, Rev. Mod. Phys. **90**, 015003 (2018).

[5] R. F. Lebed, R. E. Mitchell, and E. S. Swanson, Heavy-quark QCD exotica, Prog. Part. Nucl. Phys. **93**, 143 (2017).

[6] H. X. Chen, W. Chen, X. Liu, and S. L. Zhu, The hidden-charm pentaquark and tetraquark states, Phys. Rep. **639**, 1 (2016).

[7] A. Ali, J. S. Lange, and S. Stone, Exotics: Heavy penta-quarks and tetraquarks, Prog. Part. Nucl. Phys. **97**, 123 (2017).

[8] A. Esposito, A. Pilloni, and A. D. Polosa, Multiquark resonances, Phys. Rep. **668**, 1 (2016).

[9] Y. R. Liu, H. X. Chen, W. Chen, X. Liu, and S. L. Zhu, Pentaquark and tetraquark states, Prog. Part. Nucl. Phys. **107**, 237 (2019).

[10] F. K. Guo, C. Hanhart, U. G. Meissner, Q. Wang, Q. Zhao, and B. S. Zou, Hadronic molecules, Rev. Mod. Phys. **90**, 015004 (2018).

[11] J. P. Ader, J. M. Richard, and P. Taxil, Do narrow heavy multi - quark states exist, Phys. Rev. D **25**, 2370 (1982).

[12] Y. Iwasaki, A possible model for new resonances-exotics and hidden charm, Prog. Theor. Phys. **54**, 492 (1975).

[13] S. Zouzou, B. Silvestre-Brac, C. Gignoux, and J. M. Richard, Four quark bound states, Z. Phys. C **30**, 457 (1986).

[14] L. Heller and J. A. Tjon, On bound states of heavy $Q^2\bar{Q}^2$ systems, Phys. Rev. D **32**, 755 (1985).

[15] R. J. Lloyd and J. P. Vary, All charm tetraquarks, Phys. Rev. D **70**, 014009 (2004).

[16] N. Barnea, J. Vijande, and A. Valcarce, Four-quark spectroscopy within the hyperspherical formalism, Phys. Rev. D **73**, 054004 (2006).

[17] J. Vijande, A. Valcarce, and N. Barnea, Exotic meson-meson molecules and compact four-quark states, Phys. Rev. D **79**, 074010 (2009).

[18] M. N. Anwar, J. Ferretti, F. K. Guo, E. Santopinto, and B. S. Zou, Spectroscopy and decays of the fully-heavy tetraquarks, Eur. Phys. J. C **78**, 647 (2018).

[19] M. Karliner, S. Nussinov, and J. L. Rosner, $QQ\bar{Q}\bar{Q}$ states: Masses, production, and decays, Phys. Rev. D **95**, 034011 (2017).

[20] Y. Bai, S. Lu, and J. Osborne, Beauty-full tetraquarks, Phys. Lett. B **798**, 134930 (2019).

[21] A. V. Berezhnoy, A. V. Luchinsky, and A. A. Novoselov, Tetraquarks composed of 4 heavy quarks, Phys. Rev. D **86**, 034004 (2012).

[22] Z. G. Wang, Analysis of the $QQ\bar{Q}\bar{Q}$ tetraquark states with QCD sum rules, Eur. Phys. J. C **77**, 432 (2017).

[23] Z. G. Wang and Z. Y. Di, Analysis of the vector and axialvector $QQ\bar{Q}\bar{Q}$ tetraquark states with QCD sum rules, Acta Phys. Pol. B **50**, 1335 (2019).

[24] V. R. Debastiani and F. S. Navarra, A non-relativistic model for the $[cc][\bar{c}\bar{c}]$ tetraquark, Chin. Phys. C **43**, 013105 (2018).

[25] A. Esposito and A. D. Polosa, A $bb\bar{b}\bar{b}$ di-bottomonium at the LHC, Eur. Phys. J. C **78**, 782 (2018).

[26] P. Lundhammar and T. Ohlsson, Nonrelativistic model of tetraquarks and predictions for their masses from fits to charmed and bottom meson data, Phys. Rev. D **102**, 054018 (2020).

[27] J. M. Richard, A. Valcarce, and J. Vijande, Few-body quark dynamics for doubly heavy baryons and tetraquarks, Phys. Rev. C **97**, 035211 (2018).

[28] J. M. Richard, A. Valcarce, and J. Vijande, String dynamics and metastability of all-heavy tetraquarks, Phys. Rev. D **95**, 054019 (2017).

[29] J. Wu, Y. R. Liu, K. Chen, X. Liu, and S. L. Zhu, Heavy-flavored tetraquark states with the $QQ\bar{Q}\bar{Q}$ configuration, Phys. Rev. D **97**, 094015 (2018).

[30] C. Hughes, E. Eichten, and C. T. H. Davies, Searching for beauty-fully bound tetraquarks using lattice nonrelativistic QCD, Phys. Rev. D **97**, 054505 (2018).

[31] W. Chen, H. X. Chen, X. Liu, T. G. Steele, and S. L. Zhu, Hunting for exotic doubly hidden-charm/bottom tetraquark states, Phys. Lett. B **773**, 247 (2017).

[32] W. Chen, H. X. Chen, X. Liu, T. G. Steele, and S. L. Zhu, Doubly hidden-charm/bottom $QQ\bar{Q}\bar{Q}$ tetraquark states, EPJ Web Conf. **182**, 02028 (2018).

[33] M. S. Liu, Q. F. Lü, X. H. Zhong, and Q. Zhao, All-heavy tetraquarks, Phys. Rev. D **100**, 016006 (2019).

[34] C. Deng, H. Chen, and J. Ping, Towards the understanding of fully-heavy tetraquark states from various models, Phys. Rev. D **103**, 014001 (2021).

[35] G. J. Wang, L. Meng, and S. L. Zhu, Spectrum of the fully-heavy tetraquark state $QQ\bar{Q}'\bar{Q}'$, Phys. Rev. D **100**, 096013 (2019).

[36] M. A. Bedolla, J. Ferretti, C. D. Roberts, and E. Santopinto, Spectrum of fully-heavy tetraquarks from a diquark $+$ antidiquark perspective, Eur. Phys. J. C **80**, 1004 (2020).

[37] X. Chen, Fully-charm tetraquarks: $cc\bar{c}\bar{c}$, arXiv:2001 .06755.

[38] R. Aaij *et al.* (LHCb Collaboration), Observation of structure in the J/ψ-pair mass spectrum, Science bulletin **65**, 1983 (2020).

[39] G. Aad *et al.* (ATLAS Collaboration), Observation of an excess of dicharmonium events in the four-muon final state with the ATLAS detector, Phys. Rev. Lett. **131**, 151902 (2023).

[40] A. Hayrapetyan *et al.* (CMS Collaboration), Observation of new structure in the $J/\psi J/\psi$ mass spectrum in proton-proton collisions at $\sqrt{s} = 13$ TeV, Phys. Rev. Lett. **132**, 111901 (2024).

[41] W. C. Dong and Z. G. Wang, Going in quest of potential tetraquark interpretations for the newly observed $T_{\psi\psi}$ states in light of the diquark-antidiquark scenarios, Phys. Rev. D **107**, 074010 (2023).

[42] W. Chen, Q. N. Wang, Z. Y. Yang, H. X. Chen, X. Liu, T. G. Steele, and S. L. Zhu, Searching for fully-heavy tetraquark states in QCD moment sum rules, Nucl. Part. Phys. Proc. **318–323**, 73 (2022).

[43] R. N. Faustov, V. O. Galkin, and E. M. Savchenko, Fully-heavy tetraquark spectroscopy in the relativistic quark model, Symmetry **14**, 2504 (2022).

[44] P. Y. Niu, E. Wang, Q. Wang, and S. Yang, Determine the quantum numbers of $X(6900)$ from photon-photon fusion in ultra-peripheral heavy ion collisions, arXiv:2209.01924.

[45] G. J. Wang, Q. Meng, and M. Oka, S-wave fully charmed tetraquark resonant states, Phys. Rev. D **106**, 096005 (2022).

[46] H. T. An, S. Q. Luo, Z. W. Liu, and X. Liu, Systematic search of fully heavy tetraquark states, Eur. Phys. J. C **83**, 740 (2023).

[47] V. Biloshytskyi, V. Pascalutsa, L. Harland-Lang, B. Malaescu, K. Schmieden, and M. Schott, Two-photon decay of X(6900) from light-by-light scattering at the LHC, Phys. Rev. D **106,** L111902 (2022).

[48] J. Z. Wang and X. Liu, Improved understanding of the peaking phenomenon existing in the new di-J/ψ invariant mass spectrum from the CMS Collaboration, Phys. Rev. D **106,** 054015 (2022).

[49] C. Gong, M. C. Du, and Q. Zhao, Pseudoscalar charmonium pair interactions via the Pomeron exchange mechanism, Phys. Rev. D **106,** 054011 (2022).

[50] R. H. Wu, Y. S. Zuo, C. Y. Wang, C. Meng, Y. Q. Ma, and K. T. Chao, NLO results with operator mixing for fully heavy tetraquarks in QCD sum rules, J. High Energy Phys. 11 (2022) 023.

[51] Z. Zhuang, Y. Zhang, Y. Ma, and Q. Wang, Lineshape of the compact fully heavy tetraquark, Phys. Rev. D **105,** 054026 (2022).

[52] Y. Yan, Y. Wu, X. Hu, H. Huang, and J. Ping, Fully heavy pentaquarks in quark models, Phys. Rev. D **105,** 014027 (2022).

[53] Q. N. Wang, Z. Y. Yang, and W. Chen, Exotic fully-heavy $Q\bar{Q}Q\bar{Q}$ tetraquark states in $\mathbf{8}_{[Q\bar{Q}]} \otimes \mathbf{8}_{[Q\bar{Q}]}$ color configuration, Phys. Rev. D **104,** 114037 (2021).

[54] A. J. Majarshin, Y. A. Luo, F. Pan, and J. Segovia, Bosonic algebraic approach applied to the $[QQ][\bar{Q}\bar{Q}]$ tetraquarks, Phys. Rev. D **105,** 054024 (2022).

[55] Z. Zhao, K. Xu, A. Kaewsnod, X. Liu, A. Limphirat, and Y. Yan, Study of charmoniumlike and fully-charm tetraquark spectroscopy, Phys. Rev. D **103,** 116027 (2021).

[56] Q. Li, C. H. Chang, G. L. Wang, and T. Wang, Mass spectra and wave functions of $T_{QQ\bar{Q}\bar{Q}}$ tetraquarks, Phys. Rev. D **104,** 014018 (2021).

[57] G. J. Wang, L. Meng, M. Oka, and S. L. Zhu, Higher fully charmed tetraquarks: Radial excitations and P-wave states, Phys. Rev. D **104,** 036016 (2021).

[58] G. Yang, J. Ping, and J. Segovia, Exotic resonances of fully-heavy tetraquarks in a lattice-QCD insipired quark model, Phys. Rev. D **104,** 014006 (2021).

[59] Y. Huang, F. Feng, Y. Jia, W. L. Sang, D. S. Yang, and J. Y. Zhang, Inclusive production of fully-charmed 1^{+-} tetraquark at B factory, Chin. Phys. C **45,** 093101 (2021).

[60] V. P. Gonçalves and B. D. Moreira, Fully - heavy tetraquark production by $\gamma\gamma$ interactions in hadronic collisions at the LHC, Phys. Lett. B **816,** 136249 (2021).

[61] M. Z. Liu and L. S. Geng, Is X(7200) the heavy anti-quark diquark symmetry partner of X(3872)?, Eur. Phys. J. C **81,** 179 (2021).

[62] J. Z. Wang, X. Liu, and T. Matsuki, Fully-heavy structures in the invariant mass spectrum of $J/\psi\psi(3686)$, $J/\psi\psi(3770)$, $\psi(3686)\psi(3686)$, and $J/\psi\Upsilon(1S)$ at hadron colliders, Phys. Lett. B **816,** 136209 (2021).

[63] B. D. Wan and C. F. Qiao, Gluonic tetracharm configuration of X(6900), Phys. Lett. B **817,** 136339 (2021).

[64] C. Gong, M. C. Du, Q. Zhao, X. H. Zhong, and B. Zhou, Nature of X(6900) and its production mechanism at LHCb, Phys. Lett. B **824,** 136794 (2022).

[65] Q. F. Cao, H. Chen, H. R. Qi, and H. Q. Zheng, Some remarks on X(6900), Chin. Phys. C **45,** 103102 (2021).

[66] Z. H. Guo and J. A. Oller, Insights into the inner structures of the fully charmed tetraquark state X(6900), Phys. Rev. D **103,** 034024 (2021).

[67] R. Zhu, Fully-heavy tetraquark spectra and production at hadron colliders, Nucl. Phys. **B966,** 115393 (2021).

[68] J. R. Zhang, 0^+ fully-charmed tetraquark states, Phys. Rev. D **103,** 014018 (2021).

[69] F. Feng, Y. Huang, Y. Jia, W. L. Sang, X. Xiong, and J. Y. Zhang, Fragmentation production of fully-charmed tetraquarks at the LHC, Phys. Rev. D **106,** 114029 (2022).

[70] Y. Q. Ma and H. F. Zhang, Exploring the Di-J/ψ Resonances around 6.9 GeV Based on *ab initio* Perturbative QCD, arXiv:2009.08376.

[71] X. K. Dong, V. Baru, F. K. Guo, C. Hanhart, and A. Nefediev, Coupled-channel interpretation of the LHCb Double-J/ψ spectrum and hints of a new state near the $J/\psi J/\psi$ threshold, Phys. Rev. Lett. **126,** 132001 (2021); **127,** 119901(E) (2021).

[72] Z. G. Wang, Revisit the tetraquark candidates in the $J/\psi J/\psi$ mass spectrum, Int. J. Mod. Phys. A **36,** 2150014 (2021).

[73] M. Karliner and J. L. Rosner, Interpretation of structure in the di-J/ψ spectrum, Phys. Rev. D **102,** 114039 (2020).

[74] J. Z. Wang, D. Y. Chen, X. Liu, and T. Matsuki, Producing fully charm structures in the J/ψ -pair invariant mass spectrum, Phys. Rev. D **103,** 071503 (2021).

[75] J. F. Giron and R. F. Lebed, Simple spectrum of $c\bar{c}c\bar{c}$ states in the dynamical diquark model, Phys. Rev. D **102,** 074003 (2020).

[76] X. Y. Wang, Q. Y. Lin, H. Xu, Y. P. Xie, Y. Huang, and X. Chen, Discovery potential for the LHCb fully-charm tetraquark X(6900) state via $\bar{p}p$ annihilation reaction, Phys. Rev. D **102,** 116014 (2020).

[77] H. X. Chen, W. Chen, X. Liu, and S. L. Zhu, Strong decays of fully-charm tetraquarks into di-charmonia, Sci. Bull. **65,** 1994 (2020).

[78] H. X. Chen, Y. X. Yan, and W. Chen, Decay behaviors of the fully bottom and fully charm tetraquark states, Phys. Rev. D **106,** 094019 (2022).

[79] C. Becchi, J. Ferretti, A. Giachino, L. Maiani, and E. Santopinto, A study of $cc\bar{c}\bar{c}$ tetraquark decays in 4 muons and in $D^{(*)}\bar{D}^{(*)}$ at LHC, Phys. Lett. B **811,** 135952 (2020).

[80] C. Becchi, A. Giachino, L. Maiani, and E. Santopinto, Search for $bb\bar{b}\bar{b}$ tetraquark decays in 4 muons, B^+B^-, $B^0\bar{B}^0$ and $B_s^0\bar{B}_s^0$ channels at LHC, Phys. Lett. B **806,** 135495 (2020).

[81] Z. G. Wang, Tetraquark candidates in the LHCb's di-J/ψ mass spectrum, Chin. Phys. C **44,** 113106 (2020).

[82] G. Yang, J. Ping, L. He, and Q. Wang, Potential model prediction of fully-heavy tetraquarks $QQ\bar{Q}\bar{Q}$ ($Q = c, b$), arXiv:2006.13756.

[83] P. Niu, Z. Zhang, Q. Wang, and M. L. Du, The third peak structure in the double J/ψ spectrum, Sci. Bull. **68,** 800 (2023).

[84] Z. R. Liang and D. L. Yao, On the nature of X(6900) and other structures in the LHCb di-j/ψ spectrum, Suppl. Rev. Mex. Fis. **3,** 0308042 (2022).

[85] Z. R. Liang, X. Y. Wu, and D. L. Yao, Hunting for states in the recent LHCb di-J/ψ invariant mass spectrum, Phys. Rev. D **104,** 034034 (2021).

[86] X. K. Dong, V. Baru, F. K. Guo, C. Hanhart, A. Nefediev, and B. S. Zou, Is the existence of a $J/\psi J/\psi$ bound state plausible?, Sci. Bull. **66,** 2462 (2021).

[87] H. W. Ke, X. Han, X. H. Liu, and Y. L. Shi, Tetraquark state $X(6900)$ and the interaction between diquark and antidiquark, Eur. Phys. J. C **81,** 427 (2021).

[88] B. C. Yang, L. Tang, and C. F. Qiao, Scalar fully-heavy tetraquark states $QQ'\bar{Q}\bar{Q}'$ in QCD sum rules, Eur. Phys. J. C **81,** 324 (2021).

[89] X. Z. Weng, X. L. Chen, W. Z. Deng, and S. L. Zhu, Systematics of fully heavy tetraquarks, Phys. Rev. D **103,** 034001 (2021).

[90] J. Zhao, S. Shi, and P. Zhuang, Fully-heavy tetraquarks in a strongly interacting medium, Phys. Rev. D **102,** 114001 (2020).

[91] S. Q. Kuang, Q. Zhou, D. Guo, Q. H. Yang, and L. Y. Dai, Study of $X(6900)$ with unitarized coupled channel scattering amplitudes, Eur. Phys. J. C **83,** 383 (2023).

[92] Q. Zhou, D. Guo, S. Q. Kuang, Q. H. Yang, and L. Y. Dai, Nature of the X(6900) in partial wave decomposition of $J/\psi J/\psi$ scattering, Phys. Rev. D **106,** L111502 (2022).

[93] F. X. Liu, M. S. Liu, X. H. Zhong, and Q. Zhao, Higher mass spectra of the fully-charmed and fully-bottom tetraquarks, Phys. Rev. D **104,** 116029 (2021).

[94] E. Eichten, K. Gottfried, T. Kinoshita, K. D. Lane, and T. M. Yan, Charmonium: The model, Phys. Rev. D **17,** 3090 (1978); **21,** 313(E) (1980).

[95] Q. F. Lü, D. Y. Chen, and Y. B. Dong, Masses of fully heavy tetraquarks $QQ\bar{Q}\bar{Q}$ in an extended relativized quark model, Eur. Phys. J. C **80,** 871 (2020).

[96] W. J. Deng, H. Liu, L. C. Gui, and X. H. Zhong, Charmonium spectrum and their electromagnetic transitions with higher multipole contributions, Phys. Rev. D **95,** 034026 (2017).

[97] M. S. Liu, Q. F. Lü, and X. H. Zhong, Triply charmed and bottom baryons in a constituent quark model, Phys. Rev. D **101,** 074031 (2020).

[98] T. Barnes, N. Black, and E. S. Swanson, Meson meson scattering in the quark model: Spin dependence and exotic channels, Phys. Rev. C **63,** 025204 (2001).

[99] G. J. Wang, L. Y. Xiao, R. Chen, X. H. Liu, X. Liu, and S. L. Zhu, Probing hidden-charm decay properties of P_c states in a molecular scenario, Phys. Rev. D **102,** 036012 (2020).

[100] L. Y. Xiao, G. J. Wang, and S. L. Zhu, Hidden-charm strong decays of the Z_c states, Phys. Rev. D **101,** 054001 (2020).

[101] G. J. Wang, L. Meng, L. Y. Xiao, M. Oka, and S. L. Zhu, Mass spectrum and strong decays of tetraquark $\bar{c}\bar{s}qq$ states, Eur. Phys. J. C **81,** 188 (2021).

[102] S. Han and L. Y. Xiao, Aspects of $Z_{cs}(3985)$ and $Z_{cs}(4000)$, Phys. Rev. D **105,** 054008 (2022).

[103] F. X. Liu, R. H. Ni, X. H. Zhong, and Q. Zhao, Charmed-strange tetraquarks and their decays in a potential quark model, Phys. Rev. D **107,** 096020 (2023).

[104] F. X. Liu, M. S. Liu, X. H. Zhong, and Q. Zhao, Fully-strange tetraquark $ss\bar{s}\bar{s}$ spectrum and possible experimental evidence, Phys. Rev. D **103,** 016016 (2021).

[105] D. M. Brink and F. Stancu, Tetraquarks with heavy flavors, Phys. Rev. D **57,** 6778 (1998).

[106] D. V. Fedorov, Analytic matrix elements with shifted correlated Gaussians, Few-Body Syst. **58,** 21 (2017).